

14. MAJOR ELEMENT AND Sr ISOTOPE COMPOSITION OF INTERSTITIAL WATERS IN SEDIMENTS FROM LEG 129: THE ROLE OF DIAGENETIC REACTIONS¹

Christian France-Lanord,² Annie Michard,^{2,3} and Anne Marie Karpoff⁴

ABSTRACT

Interstitial water samples from Leg 129, Sites 800, 801, and 802 in the Pigafetta and Mariana basins (central western Pacific), have been analyzed for major elements, B, Li, Mn, Sr, and ⁸⁷Sr/⁸⁶Sr. At all sites waters show enrichment in Ca and Sr and are depleted in Mg, K, Na, SO₄, B, alkalinity, and ⁸⁷Sr compared to seawater. These changes are related to alteration of basaltic material into secondary smectite and zeolite and recrystallization of biogenic carbonate. Water concentration depth profiles are characterized by breaks due to the presence of barriers to diffusion such as chert layers at Sites 800 and 801 and highly cemented volcanic ash at Site 802.

In Site 800, below a chert layer, concentration depth profiles are vertical and reflect slight alteration of volcanic matter, either *in situ* or in the upper basaltic crust. Release of interlayer water from clay minerals is likely to induce observed Cl depletions.

At Site 801, two units act as diffusion barrier and isolate the volcanoclastic sediments from ocean and basement. Diagenetic alteration of volcanic matter generates a chemical signature similar to that at Site 800. Just above the basaltic crust, interstitial waters are less evolved and reflect low alteration of the crust, probably because of the presence in the sediments of layers with low diffusivities.

At Site 802, in Miocene tuffs, the chemical evolution generated by diagenetic alteration is extreme (Ca = 130 mmol, ⁸⁷Sr/⁸⁶Sr = 0.7042 at 83 meters below seafloor) and is accompanied by an increase of the Cl content (630 mmol) due to water uptake in secondary hydrous phases. Factors that enhance this evolution are a high sediment accumulation rate, high cementation preventing diffusive exchange and the reactive composition of the sediment (basaltic glass). The chemical variation is estimated to result in the alteration of more than 20% of the volcanic matter in a nearly closed system.

INTRODUCTION

The chemical and isotopic variations of interstitial waters extracted from deep-sea sediments from many Deep Sea Drilling Project—Ocean Drilling Program (DSDP-ODP) sites are the result of diffusive exchange between seawater and the basaltic upper crust undergoing alteration (e.g., McDuff and Gieskes, 1976). The classical pattern observed is a mole-to-mole increase of Ca and depletion of Mg. Diagenetic reactions also generate chemical variations in the interstitial waters. Volcanic ash in the sediment is commonly altered and produces a chemical pattern similar to that of alteration of basaltic upper crust (e.g., Kastner and Gieskes, 1976). The chemical depth profiles at a given site represent, therefore, the synthesis of three main processes: diffusion, diagenesis, and alteration of the basaltic crust. All are controlled by a set of more or less independent factors in the sediment: mineralogical composition, diffusive properties, chemical reactivities, sedimentation rate, porosity, permeability, and temperature.

In this paper we present the chemical and Sr isotope composition of interstitial waters sampled during Leg 129. The chemical transformations of the interstitial waters are interpreted on the basis of mineralogical, chemical, isotopic, and physical data from the sediments. Three sites (800, 801, and 802) were drilled in the Pigafetta and East Mariana basins in order to recover Jurassic sediment and oceanic crust (Fig. 1). Site 801 reached Callovian-Bathonian sediments overlying alkali and tholeiitic basalts, which are a remnant of the Jurassic superocean that once covered two-thirds of the Earth's surface. At all three sites there are thick Cretaceous volcanoclastic

sequences which are overlain at Sites 800 and 801 by siliceous layers. At these sites the influence of diffusion is considerably reduced because of the presence of a high degree of cementation. These diffusion barriers allow us to examine closely the budgets of diagenetic reactions and the chemical behavior of smectite-rich sediments. At Site 802 concentrations of most elements reach extreme values similar to those observed at several recently drilled ODP sites in Miocene-Oligocene volcanoclastic sediments (Egeberg et al., 1990a, 1990b; Collot, Greene, Stokking, et al., 1992; Parson, Hawkins, Allan, et al., 1992; Blank, 1991).

METHODS

Water samples were extracted by squeezing 5- to 10-cm-long whole-round core sections at room temperature in a titanium and stainless steel piston modified after Manheim and Sayles (1974). Shipboard analyses include pH, salinity, chlorinity, and alkalinity, and concentrations of calcium, magnesium, sulfate, potassium, strontium, silica, and manganese. Shipboard data and techniques are discussed in the *Initial Reports* (Lancelot, Larson, et al., 1990). Concentrations of Na, Mg, K, and Li were measured by atomic absorption in absorption mode, and B, complexed with carminic acid, was measured by a colorimetric method.

⁸⁷Sr/⁸⁶Sr ratios and Sr content were measured on a six-collector 262 Finnegan-Mat mass spectrometer in static mode. Sr isotope analyses were done on interstitial water samples and rock samples. Rock samples were leached with 0.5N HCl acid and rinsed with distilled water. After centrifugation, the acid leachate and first rinse were combined and dried. Part of the dried material was weighed and spiked (leachate), as was a part of the residual material (residue). Hence, rock analyses comprise analyses of (1) the leached residue (mostly silicates) and (2) the leachate where Sr is mainly released by carbonates but also by hydroxides and interstitial water salts. Chemical separation followed the technique described by Alibert et al. (1983).

On the basis of chemical composition of the drilling mud and seawater and of the period of injection of the mud during drilling, no

¹ Larson, R. L., Lancelot, Y., et al., 1992. *Proc. ODP, Sci. Results*, 129: College Station, TX (Ocean Drilling Program).

² Centre de Recherches Pétrographiques et Géochimiques—CNRS, BP 20, 54501 Vandœuvre Cedex, France.

³ Laboratoire Géosciences de l'environnement, Université St. Jérôme, C.O. 431, 13397 Marseille Cedex 13, France.

⁴ Centre de géochimie de la surface—CNRS, 1 rue de Blessig, 67000 Strasbourg, France.

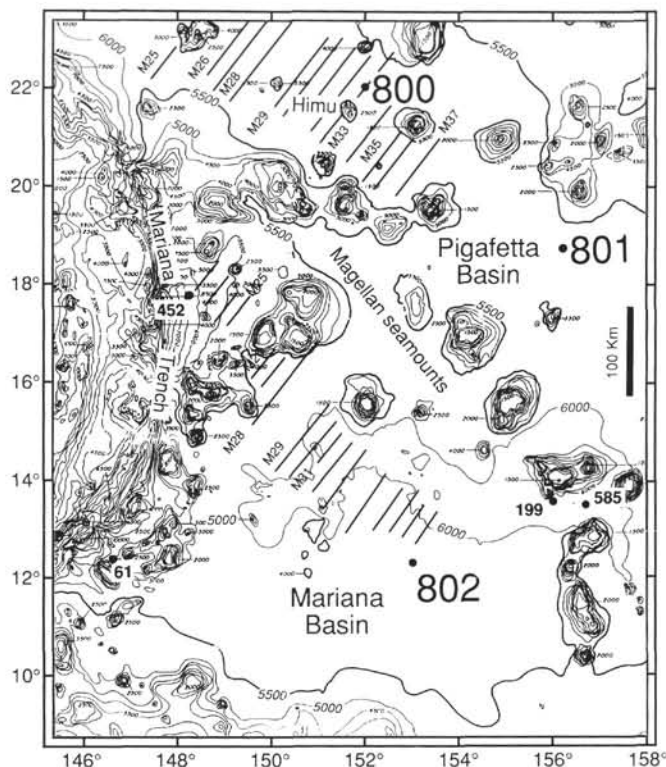


Figure 1. Location of Sites 800, 801, and 802 and DSDP sites in the area of the Pigafetta and East Mariana basins (Lancelot, Larson, et al., 1990). Bathymetry in meters. Diagonal lines denote magnetic anomalies.

contamination by seawater and/or drilling fluids is evident (Lancelot, Larson, et al., 1990). None of the observed chemical variations can be explained by the mixing of pore water with seawater or drilling fluids. Moreover, isotopic compositions of Sr and hydrogen (France-Lanord and Sheppard, this volume) show no evidence of seawater addition.

Major and trace elements analyses of solid sediment were done by ICP at CNRS-CRPG, Nancy, France (K. Govindaraju, analyst) after melting with Ce metaborate. Analyses were done on squeezed cake samples which reduce the contribution of interstitial water salts. This is especially important for Na concentrations.

SITE DESCRIPTIONS AND RESULTS

Analyses of interstitial water are given in Table 1 and shown as concentration vs. depth diagrams in Figures 2, 3, 4, and 5. Corresponding sediment lithologic descriptions and whole-rock X-ray diffraction (XRD) determinations are reported in Table 2, and major and trace element analyses of solid sediments in Tables 3 and 4, respectively.

Site 800—Pigafetta Basin

Site 800 is located at a water depth of 5686 m in the northern Pigafetta Basin near the Himu Seamount (Fig. 1). The sediments range in age from Cenozoic to Berriasian. They have been divided into five units (Fig. 2):

Unit I (0–38 m below seafloor [mbsf]): Tertiary to upper Campanian zeolitic pelagic brown clay.

Unit II (38–78 mbsf): upper Campanian to Turonian brown chert and porcellanite.

Unit III (78–229 mbsf): Cenomanian to lower Albian gray chert and silicified limestones and nannofossil chalk at the base. Porosities are low (7 to 20 vol%) at the top.

Unit IV (229–450 mbsf): Aptian volcanoclastic turbidites in sequences of interbedded clay, claystones, silty clay, silty sandstone, and sandstones. They are composed of (1) redeposited volcanic ash, with sporadic biogenic carbonates in the upper part and (2) secondary smectites, zeolites, and calcite. Volcanic material is possibly derived from the nearby Himu Seamount (Fig. 1) whose age is ≈ 120 Ma (Smith et al., 1989).

Unit V (450–498 mbsf): Hauterivian to Berriasian claystone and radiolarite.

The sediment sequence overlies massive dolerite sills.

Eight samples were squeezed, one from Unit I and seven from Unit IV and below (Table 1). Because of both the lithology and scarce recovery, no samples were taken in Units II and III. The major solute concentrations differ above and below the chert layers (Fig. 2). Concentrations at 22 mbsf are similar to seawater values. Below, in Unit IV, Na, Mg, K, SO_4 , and alkalinity concentrations are strongly reduced. Cl is also depleted to about 95% of its value in seawater. The extent of the depletion is lower at 327 and 473 mbsf. The overall trend of Ca concentration is the opposite of the other major constituents.

The Sr concentration is 3.5 times higher than in seawater at 232 mbsf and remains at similar concentrations below. $^{87}\text{Sr}/^{86}\text{Sr}$ ratios are relatively constant in Units IV and V, between 0.70635 and 0.70661. These values are significantly lower than those of 115- to 135-Ma seawater (0.7072–0.7075; Koepnick et al., 1985).

Site 801—Pigafetta Basin

Site 801 is situated within the “Jurassic magnetic quiet zone” in the central part of the Pigafetta Basin to the southeast of Site 800 (Fig. 1), at a water depth of 5674 m. The 462 m of sediments that were cored range in age from Cenozoic to Callovian and were divided into five units (Fig. 3):

Unit I (0–64 mbsf): Tertiary to Campanian pelagic brown clay.

Unit II (64–126 mbsf): Campanian to Turonian brown chert and porcellanite.

Unit III (126–318 mbsf): Cenomanian and Albian volcanoclastic turbidites with sporadic interlayers of pelagic clay, radiolarite, chert, and chalk. Turbidites are composed of volcanic ash and fragments (glass, feldspar, pyroxene, etc.) and secondary smectite, zeolite, and calcite.

Unit IV (318–443 mbsf): Valanginian to Oxfordian brown radiolarite with dark brown chert. Chert is abundant at the top and porosity is very low.

Unit V (443–462 mbsf): Callovian-Bathonian amber radiolarite and claystone. Metalliferous sediments consisting of pelagic clay, radiolarite, and hydrothermal hydroxide.

The basement consists of an upper alkali olivine basalt sequence (462–591 mbsf) and a lower tholeiitic pillow basalt sequence (462–591 mbsf). They are separated by a silicified hydrothermal deposit of hematite.

Seven interstitial water samples were squeezed, two from above chert Unit II and four below (Table 1). No samples were taken in the chert layer (Unit II). Interstitial water composition (Fig. 3) are chemically similar to modern seawater in the brown clay of Unit I. Only Si and SO_4 are significantly higher at 36 mbsf. Below Unit II, interstitial water extracted from the volcanoclastic turbidites display a general depletion in Mg, K, and Na and an enrichment in Ca. The overall depletion in cations is balanced by alkalinity, and SO_4 decreases while Cl remains constant. In Unit V, these changes are less significant than in the volcanoclastic turbidites.

The B content is high at the top of the sequence (783 μmol at 23 mbsf) compared to seawater. Below the chert the concentrations are variable between 300 and 500 μmol . Si is high (427 μmol) at 175 mbsf, where opal is abundant, and remains constant below at ≈ 200 μmol . Sr is almost constant at 260 ± 20 μmol below Unit II. The $^{87}\text{Sr}/^{86}\text{Sr}$ ratios are significantly lower than contemporaneous seawater in Unit III. In Unit V, the $^{87}\text{Sr}/^{86}\text{Sr}$ ratio of pore water at 454 mbsf is in the range of 160-Ma Jurassic seawater (0.7068–0.7073; Koepnick et al., 1990).

Table 1. Interstitial water concentration data and Sr isotope compositions.

Core, section, interval (cm)	Depth ^a (mbsf)	pH	Cl (mmol)	SO ₄ (mmol)	Alkalinity (meq)	Na ^b (mmol)	Na (mmol)	Ca (mmol)	K (mmol)	Mg (mmol)	B (μmol)	Si (μmol)	Sr (μmol)	nM (μmol)	Li (μmol)	⁸⁷ Sr/ ⁸⁶ Sr
129-800A-																
4R-2, 25-30	22	7.5	569	25.8	2.28	480	477	10.5	11.8	53.1	759	377	^c 89	2	33	
26R-2, 140-148	232	8.2	537	17.6	0.53	436		56.0	2.8	10.6			^c 321	87		
27R-1, 140-150	239	8.1	527	14.5	0.51	416	413	58.3	1.8	8.9	509	546	299	58		0.706351 ± 37
33R-6, 60-70	296	7.8	530	14.0	0.58	416	417	58.2	1.4	11.0	591	206	318	33		0.706584 ± 24
37R-2, 0-10	327	8.1	554	16.4	1.19	444	442	54.7	1.9	16.0		193	297	49		0.706607 ± 30
41R-2, 0-10	364	7.1	531	11.1	0.61	414	395	57.3	1.6	10.4	481	185	317	38		0.706618 ± 32
49R-2, 140-150	434	7.1	531	12.3	0.71	411	401	59.2	1.3	12.2	205	158	331	18	29	0.706584 ± 24
54R-2, 0-12	473	8.2	554	13.2	0.64	426	404	60.8	2.0	14.4	346	231	337	6	30	0.706568 ± 23
129-801A-																
3R-2, 145-150	23	7.5	562	29.3	2.83	483	473	10.9	11.2	52.0	783	200	^c 84	0	30	
5R-2, 145-150	44	7.6	564	37.2	2.92	496	462	12.0	11.6	53.2	715	323	^c 86	4	27	
19R-2, 65-73	175	8.0	560	19.3	0.72	449	452	53.2	3.8	18.4	316	427	253	51	17	0.706455 ± 22
129-801B-																
5R-2, 0-10	233	7.7	569	16.1	0.46	453	460	56.1	2.7	15.1	508	249	281	97	13	0.706383 ± 24
8R-3, 115-125	265	8.1	543	16.8	0.64	441	436	46.6	2.4	18.6	315	233	238	123	13	0.706634 ± 11
33R-1, 143-150	444	7.5	586	17.5	1.37	465	445	40.9	1.9	35.3	485	212	276	28		0.707013 ± 19
35R-2, 0-10	454	7.9	572	21.0	1.28	458	452	40.4	2.0	36.0	324	218	^c 280	25	26	
129-802A-																
4R-1, 140-150	26	7.8	554	26.8	1.36	484	477	16.2	12.2	38.6	736	162	91	6	22	0.708022 ± 39
6R-2, 0-10	44	8.3	547	36.5	0.75	492	489	42.3	11.0	15.4	433	78	135	13	6	0.706055 ± 28
10R-2, 140-150	83	9.0	631	0.4	0.57	377	354	125.2	2.7	0.5	43	194	352	19	6	0.704271 ± 18
13R-1, 53-58	109	7.8	627	3.7	0.54	362	344	130.2	2.1	4.3	111	197	283	22	7	0.704330 ± 30
19R-2, 107-117	162	8.5	610	9.9	0.60	402	388	108.3	2.1	3.9	308	157	468	16	6	0.705835 ± 27
21R-1, 103-110	179	8.4	613	11.9	0.58	398	381	114.3	1.7	3.6	315	124	^c 459	11	6	
26R-1, 0-10	225	8.1	612	12.2	0.44	390	388	118.4	1.8	2.9	324	151	487	20	11	0.706172 ± 25
29R-3, 29-34	258	7.2	584	12.0	0.62	360	363	115.5	1.9	4.7	370	913	^c 473	41	22	
32R-2, 140-150	286	6.5	576	12.5	0.23	375		96.1	4.6	12.9		637	399	46		0.706711 ± 28
36R-1, 80-88	322		614			423	423	81.8	3.9	11.8			350			0.707096 ± 27
40R-2, 140-150	361	8.0	598	15.0	0.58	430	413	80.5	2.6	10.4	386	499	294	34	26	0.707002 ± 23
43R-1, 140-150	384	7.9	579	15.1	0.58	425	415	77.3	2.5	12.1	282	556	303	48	23	0.707088 ± 20
47R-2, 140-150	422	7.9	530	13.2	0.62	396	394	66.8	2.2	11.6	270	203	260	53		0.706916 ± 20
50R-2, 140-150	450	7.9	553	13.6	0.80	406	409	74.0	2.2	10.7	668	179	284	54		0.706988 ± 23
53R-1, 120-130	471		557			388	395	68.9	2.5	12.5	336	652	265	20	11	0.707095 ± 19
56R-2, 140-150	500	8.2	586	15.7	0.80	446	443	81.5	1.2	2.9	318	216	241	22	10	0.706920 ± 23

Notes: Most pH, Cl, SO₄, alkalinity, Ca, Mg, K, Si, and Mn data are shipboard analyses (Lancelot, Larson, et al., 1990). Mean value of ⁸⁴Sr spiked NBS 987 is 0.710219 ± 18.

^aDepths rounded to the nearest meter.

^bCalculated by charge balance.

^cAnalyzed by atomic absorption rather than by isotope dilution.

Site 802—East Mariana Basin

Site 802 is in the center of the East Mariana Basin, more than 300 km from any known seamounts or island arc (Fig. 1). The water depth is 5674 m. The sediment sequence is 500 m thick and consists of redeposited material. It has been divided into nine units (Fig. 4):

Unit I (0-15 mbsf): Neogene brown clay.

Subunits IIA and IIB (15-254 mbsf): Miocene to Eocene tuff with indurated, well-preserved hyaloclastites and volcanic ash. Between 15 and 160 mbsf (Subunit IIA) the tuffs are well cemented. They are intercalated with a few layers of pelagic clay, and in the lower half they are mixed with chalk. Secondary minerals include smectites and zeolites and can range from 10% to 90% of the rock. Horizontal fractures of thaumasite (Ca₃ Si(OH)₆ CO₃ SO₄, 12H₂O), pure or mixed with zeolite, are common at the top. The mineralogy is fully described in Karpoff et al. (this volume).

Unit III (254-330 mbsf): upper Paleocene nannofossil chalk, probably redeposited as a gravity flow.

Unit IV (330-348 mbsf): Maestrichtian zeolitic pelagic claystone.

Unit V (348-460 mbsf): Campanian volcanoclastic turbidites with claystone, porcellanite, and debris flow.

Units VI to IX (460-509 mbsf): Cenomanian to upper Albian brown claystone, radiolarian limestone, and volcanoclastic turbidites.

The basement consists of remarkably fresh extrusive basalt.

Interstitial water samples were squeezed from sediment cores at 16 depths between 26 and 500 mbsf (Table 1). The depth profiles

show a clear break between 26 and 83 mbsf, with extremely large increases in Ca, Cl, pH, and Sr, and a strong decrease in ⁸⁷Sr/⁸⁶Sr ratios, Mg, K, Na, SO₄, alkalinity, B, and Li. Below, the compositions are generally constant (Figs. 4 and 5). From 258 to 500 mbsf, the trend is a progressive decrease of salinity (about 39‰ to 34‰) due to decreases in Ca and Cl contents. In this interval, Na and Mg contents increase slightly.

Pore-water ⁸⁷Sr/⁸⁶Sr ratios (Fig. 5) reach a minimum of 0.70427 at 83 mbsf. This value is similar to the ⁸⁷Sr/⁸⁶Sr ratios of both the silicate and leachable fractions of the solid sediment (Table 5 and Fig. 5). Below, the pore-water ⁸⁷Sr/⁸⁶Sr ratios increase progressively to 0.707 at 322 mbsf, in the chalk of Unit III. At 322 mbsf the ⁸⁷Sr/⁸⁶Sr ratio of carbonate is similar to that of contemporaneous seawater. From 361 to 500 mbsf, the ⁸⁷Sr/⁸⁶Sr ratios of pore waters and leachable fraction are almost constant around 0.7070, which is lower than ⁸⁷Sr/⁸⁶Sr ratios of contemporaneous seawater.

These concentrations and isotopic compositions are very unusual. For all of the DSDP-ODP sites, only several recent legs report comparable concentration gradients in volcanoclastic formations: Leg 126 (Sites 792 and 793; Egeberg et al., 1990b), Leg 134 (Sites 832 and 833; Collot, Greene, Stokking, et al., 1992), and Leg 135 (Site 841; Parson, Hawkins, Allan, et al., 1992; Blanc et al., 1991). The characteristics that these sites have in common with Unit II at Site 802 are the age, the fresh volcanoclastic compounds, and the high sedimentation rates. The main difference is the geodynamic context, which is forearc or intra-arc for Legs 126, 134, and 135.

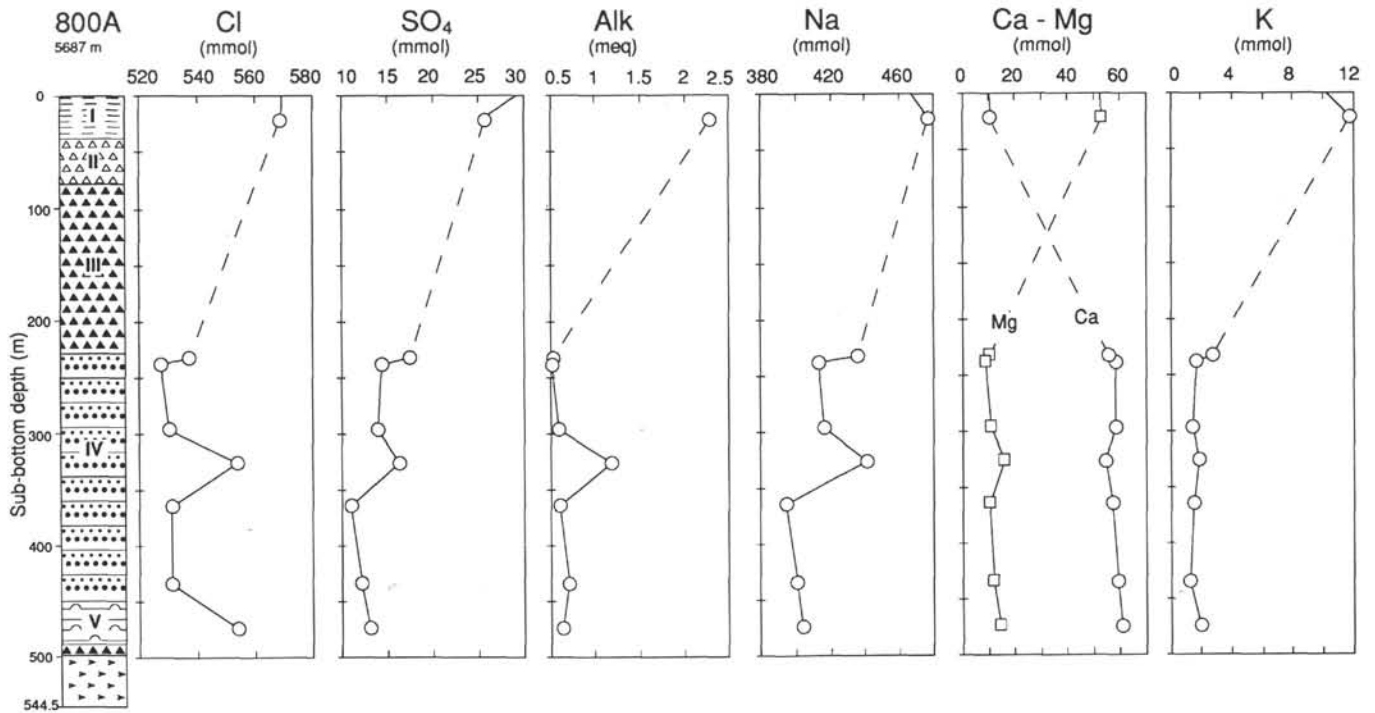


Figure 2. Distribution with depth of chloride, sulfate, alkalinity, sodium, calcium, magnesium, potassium, silica, manganese, boron, lithium, strontium, and ⁸⁷Sr/⁸⁶Sr in pore fluids of Site 800. The contemporaneous seawater curve for the Sr isotope ratio is drawn after Koepnick et al. (1985). Lithologic legend in Figure 4.

DISCUSSION

At all sites the interstitial water depth profiles present the classical depletion in Mg, K, Na, SO₄, and alkalinity, and enrichment in Ca. This variation with depth has been described at numerous DSDP-ODP sites. It results from the superimposed effects of (1) diffusion between upper crustal basalts undergoing alteration, and (2) *in-situ* reactions of volcanogenic sediment to clays and zeolites (e.g., Kastner and Gieskes, 1976; McDuff, 1981). At these three sites, the ⁸⁷Sr/⁸⁶Sr ratios of interstitial water are always lower than those of contemporaneous seawater except for the topmost samples and the bottom one at Site 801 (Fig. 3). Low ⁸⁷Sr/⁸⁶Sr ratios confirm the major role of basaltic alteration. In both cases reactions of basaltic material, which is altered to smectites and zeolites (phillipsite and clinoptilolite), are involved. These reactions release Ca and consume Mg, Na, and K from the interstitial water. Similar secondary mineralogy and chemical variation of pore waters are observed on experimental alteration of basalts at low temperature (e.g., Crovisier et al., 1987; Crovisier, 1989). The interstitial water chemistry of each site provides evidence for specific processes involving alteration of basaltic matter either within the sediments or in the underlying basalts, and other diagenetic reactions.

We examine the Sr budget on the basis of two main processes: (1) volcanic Sr release during alteration, which tends to lower the Sr isotope ratio, and (2) dissolution/recrystallization of biogenic tests, which releases Sr with an isotopic ratio of seawater contemporaneous to that of the sediment. The volcanic contribution to the Sr budget can be estimated from Sr isotope ratios of contemporaneous seawater and volcanic material (Hawkesworth and Elderfield, 1978):

$$f_{\text{volcanic}} = \frac{(^{87}\text{Sr}/^{86}\text{Sr})_{\text{seawater}} - (^{87}\text{Sr}/^{86}\text{Sr})_{\text{interstitial}}}{(^{87}\text{Sr}/^{86}\text{Sr})_{\text{seawater}} - (^{87}\text{Sr}/^{86}\text{Sr})_{\text{volcanic}}} \times 100 \quad (1)$$

The input of biogenic Sr can be estimated from the Sr content budget:

$$\sum \text{Sr}_{\text{interstitial}} = \text{Sr}_{\text{seawater}} + \text{Sr}_{\text{volcanic}} + \text{Sr}_{\text{biogenic}} \quad (2)$$

The biogenic contribution to Sr is, therefore,

$$f_{\text{biogenic}} = \frac{\sum \text{Sr} - \text{Sr}_{\text{seawater}} - (f_{\text{volcanic}} \times \sum \text{Sr})}{\sum \text{Sr}} \times 100. \quad (3)$$

Site 800

Distinctive features of the concentration profiles from Site 800 are (1) the break in slope at the chert and porcellanite unit and (2) the low chlorinity of most samples from the volcanoclastic unit. The changes in gradients are certainly due to the presence of the chert, which reduces diffusional communication. The chert unit corresponds to logging Unit 1, characterized by 6- to 9-ohm-m resistivities, which are high compared with those of other formations (0.5 to 3 ohm-m in lithologic Units III and IV) (see "Downhole Measurements" section, "Site 800" chapter, Lancelot, Larson, et al., 1990). Chert porosity is 10%-30%, whereas it is 30%-60% in the volcanoclastic sediments ("Physical Properties" section, "Site 800" chapter, 1990). Both high resistivity and low porosity imply a low diffusion constant in this unit. These results confirm the role of lithologic barriers to diffusion, which was already described for similar examples of chert over volcanoclastic units (DSDP Sites 315 and 317—Gieskes, 1976; DSDP Site 462—Gieskes and Johnson, 1981).

Diagenesis or Diffusion from the Basaltic Crust?

Under the chert barrier the interstitial water concentrations result from the combined effect of diffusion from basaltic crust and *in-situ* diagenetic reactions. The existence of *in-situ* reactions is indicated by two observations:

1. Unit IV is composed mainly of fresh and altered volcanoclastic material, including glass, which is unstable (e.g., Gislason and Eugster, 1987). Authigenic smectites and zeolites (phillipsite and clinop-

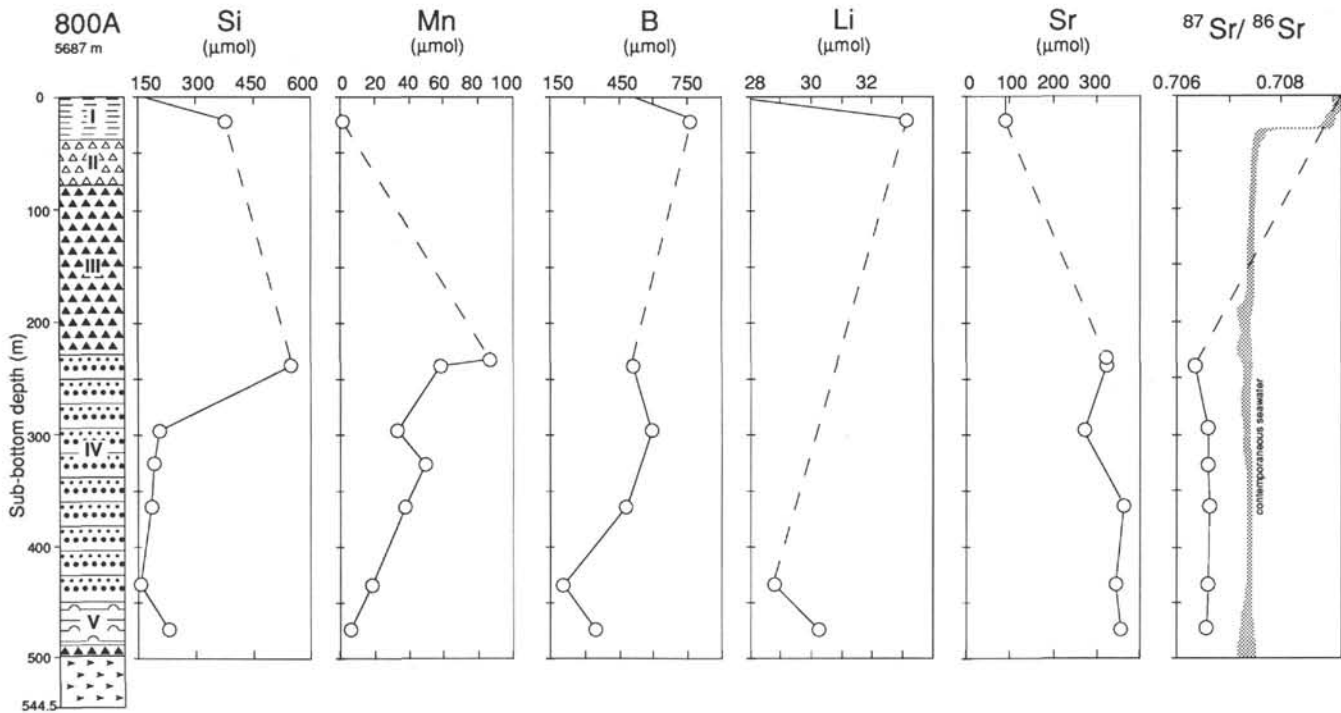


Figure 2 (continued).

tilolite) are abundant (Karpoff, this volume). The formation of such minerals from volcanic minerals (pyroxene, plagioclase, etc.) or glass consumes Mg, Na, and K and releases Ca. In this case the alkalinity sink results from calcite precipitation in response to the increase in Ca concentration. Such reactions also lower the $^{87}\text{Sr}/^{86}\text{Sr}$ ratio of interstitial water, as volcanic Sr with a low $^{87}\text{Sr}/^{86}\text{Sr}$ ratio is released (e.g., Hoffert et al., 1978).

2. The concentration profiles are not straight, contrary to what is expected for nonreacting sediments. Concentrations of Na, SO_4 , Cl, and, to a lesser extent, Mg, and K are significantly less depleted at 232, 327, and, for some elements, 473 mbsf. The Ca and Sr contents are lower at 232 and 327 mbsf. This is correlated with mineralogical and chemical differences in the sediments. At 232 and 473 mbsf, quartz is more abundant, with SiO_2 at 64.7 and 81.2 weight percent (wt%), respectively, instead of 43 to 53 wt%, as in the rest of the sequence (Table 3). The observed mineralogy is not, however, completely consistent with the Na profiles. Interstitial waters below 327 mbsf are the most depleted in Na. If we correct the depletion for a possible effect of dilution by low-salinity water (see the following discussion), the decrease in Na is approximately 20 mmol/L with respect to seawater. Na loss is usually due to Na-zeolite formation; however, zeolites have not been detected by XRD analysis in these samples (Table 2). Karpoff (this volume) reports a minor occurrence of clinoptilolite in the upper section of the unit. The observed chemical trends may correspond only to very minor changes in the mineralogy of the sediment (e.g., Egeberg et al., 1990a). The observed depletion of Na could result from the neoformation of only 1 to 5 wt% of zeolite, depending on the exact stoichiometry of the reaction and the porosity. A small amount of zeolite could be difficult to observe by XRD. The Na profile may also be the result of diffusion from the basaltic crust, as pore waters from basaltic crust are depleted in Na (Mottl and Gieskes, 1990).

Sr Budget

For the samples of the volcanoclastic sediments of Site 800, f_{volcanic} varies between 19 and 25 mol% for a volcanic ratio of 0.7035.

Figure 6 shows that the Sr content is higher than can be predicted for a simple model of dissolution of basalt in seawater. The Cretaceous Sr content of seawater is not known (e.g., Holland, 1978), which adds a major uncertainty to budget calculations. Assuming that the initial Sr content of the interstitial water was 85 μmol , f_{biogenic} should be around 50 mol% (i.e., 150 μmol is biogenic). This is a minimum estimate because the Sr uptake in secondary smectites is not included. The minimum amount of carbonate recrystallization can be calculated. Manheim and Sayles (1974) estimate that biogenic carbonates lose about 1000 parts per million (ppm) Sr as a consequence of recrystallization. Therefore, in a sediment with 25 wt% interstitial water, the 150 μmol Sr of biogenic origin requires the recrystallization of ≈ 0.5 wt% calcite in the solid sediment. This is compatible with the CaCO_3 content in the sediment between 229 and 434 mbsf (0.5 to 10 wt%, Table 4; "Site 800" chapter, Lancelot, Larson, et al., 1990). In the radiolarite of Unit V, the CaCO_3 content is less than 0.2 wt%; however, recrystallization of this small concentration could still produce a biogenic fraction of 50 mol% because of the low pore-water content (<5 wt%).

Chlorine Depletion

Four of the five samples from Unit IV are depleted in Cl by about 6% with respect to seawater. The chloride ion is conservative in marine sediments because there are no significant sinks or sources (e.g., Sayles and Manheim, 1975). Contamination by drilling mud being excluded, such a depletion is due to dilution by low-chlorinity water. Sources of fresh water are probably local because the depletion is not uniform in the Unit IV. Several sources may be proposed:

1. Dehydration related to diagenetic reactions such as organic matter degradation, smectite to illite reaction, gypsum to anhydrite conversion, or opal-A/opal-CT/quartz transitions. Based on the mineralogical composition of Unit IV, none of these reactions is likely to produce sufficient amounts of water in this context. Illite is not observed by XRD in this unit (Karpoff, this volume) and temperatures of Unit IV (10°–18°C; A. Fisher, pers. comm., 1991) are too low for

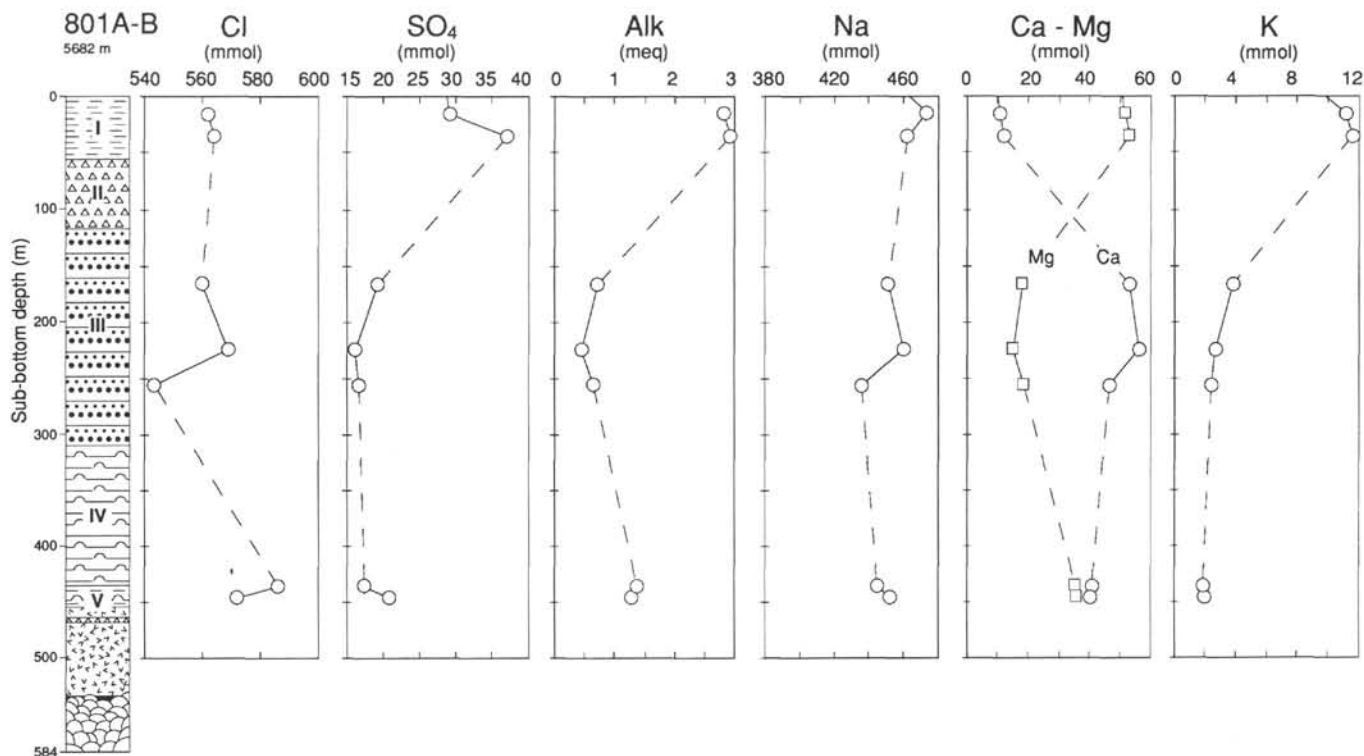


Figure 3. Distribution with depth of chloride, sulfate, alkalinity, sodium, calcium, magnesium, potassium, silica, manganese, boron, lithium, strontium, and $^{87}\text{Sr}/^{86}\text{Sr}$ in pore fluids of Site 801. The contemporaneous seawater curve for the Sr isotope ratio is drawn after Koepnick et al. (1985, 1990). Lithologic legend in Figure 4.

this type of reaction (Dunoyer de Segonzac, 1970). Opal-A/opal-CT/quartz transitions are unlikely because silica phases are rare in Unit IV (Karpoff, this volume); moreover, the levels where SiO_2 is abundant (232 and 473 mbsf) do not show significant Cl depletions.

2. Ion filtration processes could retain chloride ions in a clay-rich formation and produce low-chlorinity water (Hanshaw and Coplen, 1973), which could percolate into the sampled area. This seems unlikely because no Cl-rich waters have been observed.

3. Interlayer water expulsion under burial compaction from smectite-type minerals (e.g., Burst, 1976; Bird, 1984). This process is difficult to demonstrate, as there are no verifiable measurement of sorbed water. The effect of interlayer dewatering on pore water depends on the porosity and on the interlayer water content of the clay. For example, to generate the measured freshening (560 to 530 mmol Cl) it would be necessary to release 8.5 g $\text{H}_2\text{O}/\text{kg}$ of sediment for a pore-water content of 15 wt% and 20 g $\text{H}_2\text{O}/\text{kg}$ for a pore-water content of 35 wt%. The interlayer water content of smectite (i) is difficult to determine. According to Bird (1984) it is variable with confining pressure and temperature. In the conditions of Unit IV it can be estimated to be between 15 and 20 dry wt%. Figure 7 illustrates the relative loss of interlayer water necessary to freshen pore water by 6% as a function of the final pore-water content. This calculation is for sediment with 90 wt% smectite, and i has been fixed at 15 and 20 dry wt% (Bird, 1984; Newman, 1987, chapter 5, p. 257).

This process is strongly dependent on the porosity. Estimates of pore-water contents have been made for two smectite-rich samples on the basis of measurement of total water content (pore water + interlayer water + adsorbed water) (France-Lanord and Sheppard, this volume). The estimates of pore-water content are 42.7–40.4 wt% at 327 mbsf and 23.7–20.6 wt% at 364 mbsf, assuming values of $i = 15$ and 20% dry wt%, respectively, and 90 wt% of smectite in the sediment. A 6% chlorinity decrease would require a release of 7%–10% of the initial interlayer water at 364 mbsf and 18%–21% at 327 mbsf (Fig. 7).

In this context, the dewatering of interlayer water of smectite is a likely source of fresh water. Small losses of interlayer water (5%–10%) may explain the decrease in Cl content of interstitial water in samples that are smectite-rich and have low porosity. At 327 mbsf the porosity is too high and no decrease of Cl concentration is observed. At 232 and 473 mbsf, where SiO_2 is more abundant (64.7 and 81.2 wt%, Table 3), the chlorinity reduction is only 4% and 1.5%, respectively. This process is not frequently observed in similar deep-sea sediments; it has been proposed for ODP Site 765 (Ludden, Gradstein, et al., 1990) and inferred as a deep source of fresh water in the Barbados accretionary complex (Tribble, 1990; Gieskes et al., 1990; Vrolijk et al., 1991). At Site 800, the chert of Unit III prevents diffusion, which helps to maintain the differences in concentration. This, combined with a relatively low pore-water content (10–15 wt%) and high smectite content, is a factor in increasing the effect of the reaction.

Site 801

Diffusion Barriers and Alteration of the Jurassic Crust

Interstitial water depth profiles at Site 801 are far from simple diffusion profiles. Between 0 and 300 mbsf the chemical change is relatively similar to that at Site 800. A change in slope for nearly all chemical profiles occurs between Units I and III, which are separated by 60 m of chert-rich sediments. Low diffusion constants in the chert are indicated by the high sediment resistivities (2 to 10 ohm-m) and low porosities (8%–20%) (see "Physical Properties" and "Downhole Measurements" sections, "Site 800" chapter, Lancelot, Larson, et al., 1990). Interstitial water in the volcanoclastic Unit III is depleted in Mg, K, SO_4 , alkalinity, B, and Li, and enriched in Ca and Sr. The $^{87}\text{Sr}/^{86}\text{Sr}$ ratios are also lowered compared with that of contemporaneous seawater. The volcanic contribution to Sr is estimated to be at 20 to 25 mol% (Fig. 6). All of these compositions are typical of an alteration reaction of material of basaltic origin.

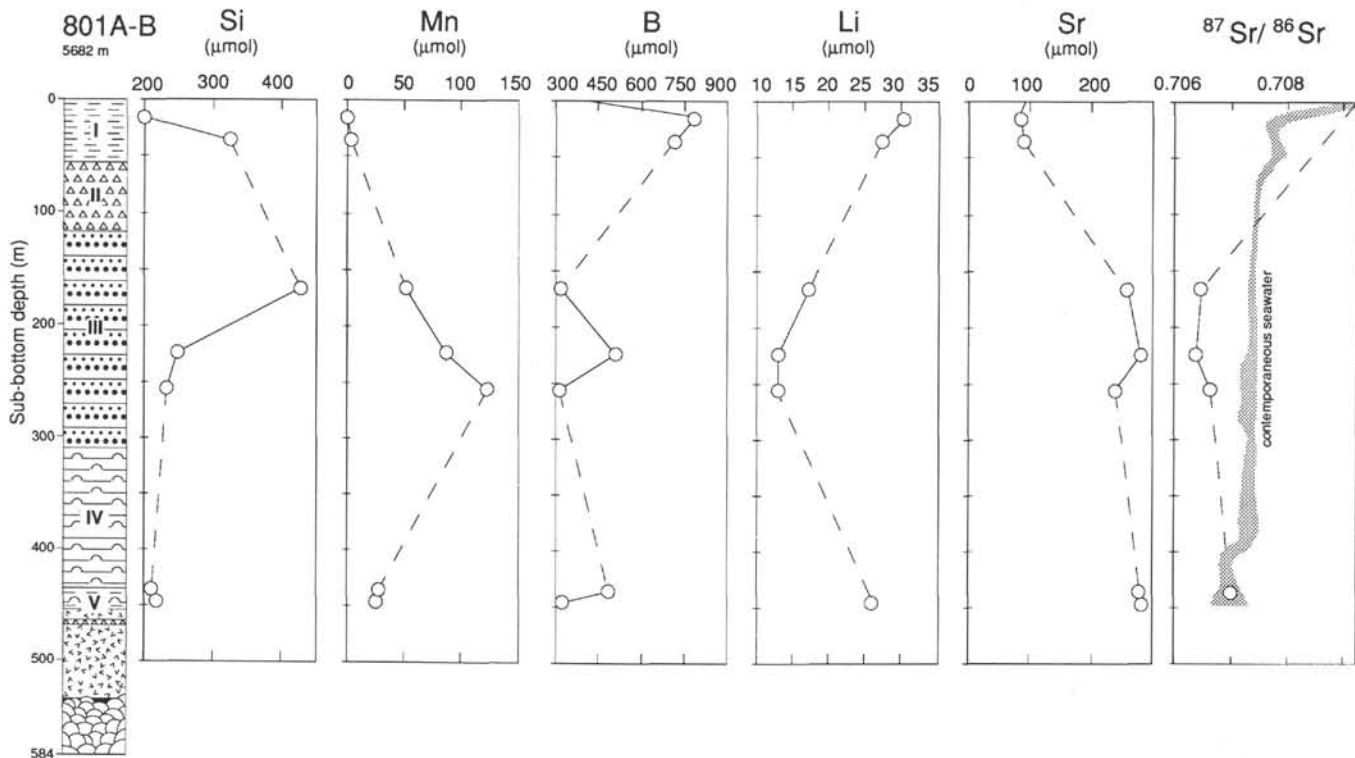


Figure 3 (continued).

From Units III to V, there is a reverse evolution of Ca, Mg, and alkalinity contents and the Sr isotope ratio. The waters in Unit V are less modified compared to seawater than those in Unit III. This change in gradients between Units III and V is important because, first, it implies that the interstitial water chemistry in volcanoclastic Unit III is mainly controlled by *in-situ* reactions rather than by diffusion from the basement. Second, the small effect of volcanic alteration on interstitial waters only 50 m above the basement suggests that the basaltic crust is not undergoing active low-temperature alteration. The petrographic and geochemical study of the underlying basalts (Alt et al., this volume) shows that significant alteration is limited to the alkali basalts and the upper 20 m of the tholeiitic basalts and is mainly related to low-temperature hydrothermal circulation. Below 540 mbsf the basalts are remarkably fresh. For instance, the H_2O^+ content of the basalts never exceeds 1.5 wt%, and the $\delta^{18}O$ values of the whole-rock basalts are between 6‰ and 8‰, little enriched in ^{18}O (e.g., Muelenbach, 1986). Based on a positive covariation between age and $\delta^{18}O$ of deep-sea basalts, Muelenbach (1980, 1986) concluded that low-temperature alteration is a continuous process and persists even after sediment deposition. This has been confirmed by the interstitial water chemistry in sediments (Lawrence and Gieskes, 1981). At Site 801, the restricted diffusion through the sediments may partially explain the limited aging alteration of the basalts. In addition to the chert of Unit II, the radiolarite of Unit IV is a thick barrier for diffusion. Especially between 330 and 400 mbsf, relatively low porosities (2.5 to 10 vol%) and high resistivities (≈ 5 ohm-m) have been measured ("Site 801" chapter, Lancelot, Larson, et al., 1990).

Diagenetic Reactions

Interstitial waters in Unit III are almost isolated by their position between the chert and the radiolarite; hence, their chemistry is principally controlled by diagenetic reactions. The chemical changes of major ions is broadly similar to what is observed in the Site 800 volcanoclastic sediments. The main differences are (1) the Na concen-

trations are constant indicating that Na is not incorporated in the secondary phases, and (2) the stability of Cl in Unit III except for a slight dip at 265 mbsf (543 mmol). The mineralogy of secondary minerals is also different from that of Unit IV of Site 800 (Table 2). Here, zeolites are rare and celadonite is dominant with smectite. At 175 and 233 mbsf, celadonite and/or opal are dominant (Tables 2 and 3); hence, interlayer water release cannot have a reduced salinity. It is only at 265 mbsf, where smectite is dominant, that a slight freshening of pore water is observed.

In Unit III the volcanic Sr represents 20 to 25 mol% of the total Sr and the Sr budget implies a biogenic carbonate contribution (Fig. 6). The $CaCO_3$ content of the sediment is 4–8 wt%, which is much higher than required by the preceding carbonate recrystallization model. In Unit V the volcanic Sr contribution is negligible, –3.5 to 4 mol% depending on the Sr isotope ratio of the contemporaneous seawater. The absence of volcanic contribution is consistent with the absence of volcanic detritus in the sediment, the red clay being of authigenic origin (Karpoff, this volume). Assuming a Sr concentration of 85 μmol for Jurassic seawater, the Sr concentration implies a Sr input of ≈ 200 $\mu\text{mol/L}$. The $CaCO_3$ content of the sediment (<0.2 wt%) is too low to account for Sr input by carbonate recrystallization. Sr may be released by dissolution of radiolarite tests, such as *Acantharia*, which contain Sr (Odum, 1951). An alternative is that Sr is released from authigenic smectite during diagenetic modifications with increasing burial and age (Clauer et al., 1975; 1982).

Site 802

The concentration gradients in the first hundred meters of Hole 802A are among the highest ever recorded in a DSDP-ODP hole. Between 44 and 83 mbsf, both Cl and Ca increase by 83 mmol/L, SO_4 , Mg, K, B, and Li are reduced to almost zero, and the $^{87}Sr/^{86}Sr$ ratio drops down to 0.704. Mechanisms that can raise the Cl concentration in interstitial waters are the dissolution of evaporites, ultrafiltration and the uptake of water in secondary minerals, or formation

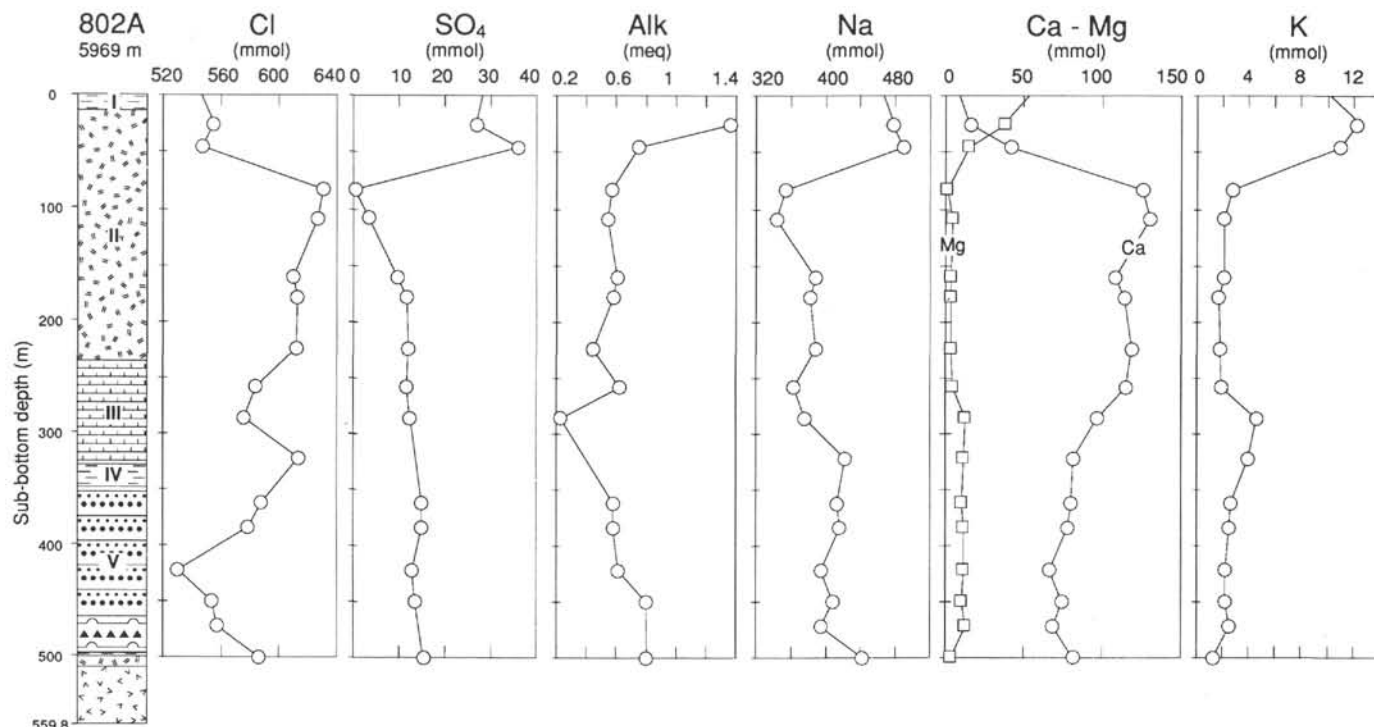


Figure 4. Distribution with depth of chloride, sulfate, alkalinity, sodium, calcium, magnesium, potassium, pH, silica, manganese, boron, and lithium in pore fluids at Site 802.

of gas hydrates. The parallel evolution of the other ions, the Sr isotope ratios, the volcanic nature of the primary material, and the secondary paragenesis rich in smectites and zeolites clearly indicate that alteration of volcanic ash into secondary hydrous minerals is the process that enhances the Cl content by water uptake. Analogously high Cl and Ca concentrations recently found at Sites 792 and 793 has been attributed to alteration reactions in the volcanoclastic sediments (Egeberg et al., 1990a).

Concentrations reach high and low extremes at 80–100 mbsf and reversed evolution are observed below this level, just below the Miocene tuffs. This implies that significant diagenetic reactions are only active in the tuff between 50 and 100 mbsf. Below the tuff, most concentration profiles are constant and similar to what is observed in volcanoclastic units at Sites 800 and 801. The fact that the $^{87}\text{Sr}/^{86}\text{Sr}$ ratios of the interstitial waters and the leachate fraction (mainly carbonates) in volcanoclastic Unit V are similar, and that the values are lower than that of contemporaneous seawater (Fig. 5), imply an equilibrium of carbonates with altered pore waters.

Closed System Evolution?

In the 40 to 80 mbsf interval, the concentration gradients are extremely high, up to 2.3 mmol/m for Ca and Cl (Fig. 4). The existence of high gradients in 10- to 15-m.y.-old sediments implies either (1) that reactions are going on rapidly now (but there is no reason why alteration should have started only recently) or (2) that the tuffs rapidly become a "closed system" because of the high accumulation rate and high cementation of the sediments, which limit diffusive transport. Overall sedimentation rates in the Miocene tuffs are at least 25 m/m.y. ("Site 802" chapter, Lancelot, Larson, et al., 1990) which is not especially high. However, the type of deposit, mass flows intercalated by pelagic intervals (Cores 129-802A-13R and -19R), suggests that accumulation rates were higher between pelagic deposition periods. No downhole measurements are available for evaluating diffusion properties in the upper 100 mbsf. Nevertheless, between 100 and 140 mbsf resistivities are highly variable between 2 and 200 ohm-m at

121–124 mbsf ("Site 802" chapter, Lancelot, Larson, et al., 1990). These high resistivity levels correspond to intervals of coarse sandy tuff well cemented by silicates. At the same level, sonic velocities reach 4 km/s. This is much higher than the mean for all sandstone and tuff samples collected during Leg 129 (2.5 to 2.8 km/s; Fisher et al., this volume) and also indicates a high degree of cementation. Intervals with a low diffusion constant are therefore likely in the upper part of the unit because a similar lithology is present.

Alteration Budget

Following Egeberg et al. (1990a) it is possible to estimate the degree of alteration of the sediment from the Cl increase, assuming that Cl is not incorporated in the minerals and that the system is closed. Such a crude estimate depends on (1) the water content of the secondary phases (assumed to be between 20 and 26 wt% for a mixture of smectite and zeolites) and (2) the initial porosity. This last parameter is related to the degree of alteration and to the final porosity. The shipboard measurements of the sediment water content between 25 and 235 mbsf is 22 to 59 wt% (average = 32 wt%). These data overestimate the real interstitial water content because all or part of the interlayer water of smectites and the channel water of zeolites is included in the measure. If smectites and zeolites represent about 20 wt% of the solids, the overestimate may reach 5 wt% of the sediment. A reasonable value for average interstitial water content is, therefore, 28 wt% and the upper limit is 40 wt%. Figure 8 shows the relation between the degree of alteration and the Cl content of the interstitial water for interstitial water contents at 25 and 40 wt% and water contents in the secondary minerals of 20 and 26 wt%. Taking into account the large uncertainties, an increase of 85 mmol of the Cl content could be achieved by the alteration of 20 to 50 wt% of the solids, with the most plausible values at about 20 wt%. This is consistent with the shipboard core descriptions, which estimate the proportion of smectite, zeolite, and calcite at 20% of the tuffs. This estimate represents the average alteration of Unit II, but at a specific level secondary minerals may represent anywhere from 5% to 95%

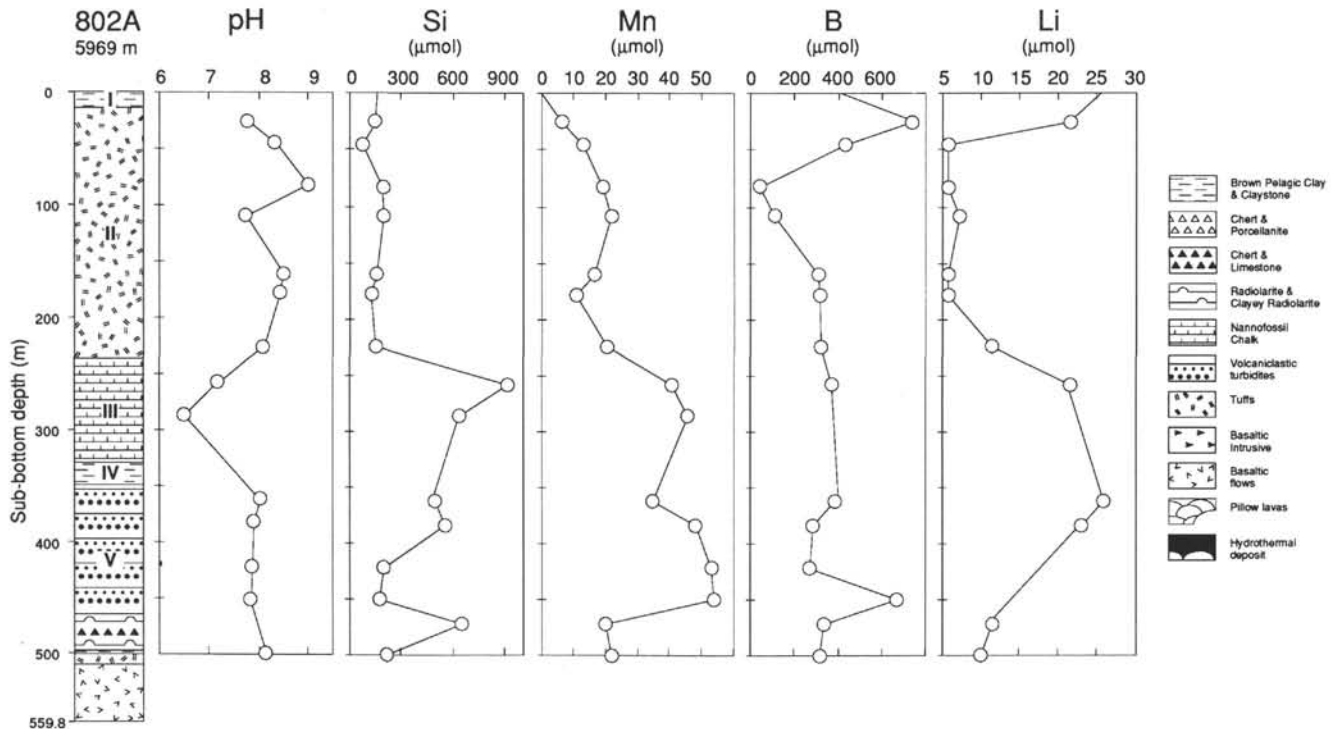


Figure 4 (continued).

of the sediment. For instance, at 83 mbsf only magnetite is visible by XRD determination and basaltic glass is certainly higher than 80% (Table 2). The consistency of the calculated degree of alteration and the observed proportion of altered minerals supports the hypothesis that Unit II behaves like a nearly closed system and that the water/rock ratio remains very low. The conditions for such a sedimentary system are high accumulation rates and low diffusion properties.

The upper part of Unit II (<110 mbsf) is depleted in Sr compared with the curve for basalt dissolution (Fig. 6). This may be due to lower concentration of Sr in Miocene seawater and/or of the $^{87}\text{Sr}/^{86}\text{Sr}$ ratio of volcanic matter. For a system with considerable volcanic contribution, the $^{87}\text{Sr}/^{86}\text{Sr}$ ratio of volcanic matter is very important. In the absence of direct measurement of the source, it has been fixed at 0.7035. This is already a little lower than the value of 0.7038 measured for the silicate fraction of Sample 129-802A-10R-2, 140–150 cm (83 mbsf), where fresh basaltic glass is dominant. Therefore, if the initial Sr concentration was similar to that of modern seawater, the low Sr content at 83 and 109 mbsf implies that Sr is incorporated in secondary phases. The phases that take up Sr in the unit are probably smectite and carbonate. At 109 mbsf the whole-rock Sr concentration is very high (1484 ppm); however, the phase(s) that contains Sr has not been identified. Below 110 mbsf, the volcanic contribution starts to decrease and the Sr content continues to increase (Fig. 6). This is consistent with the progressive increase of the CaCO_3 content of the sediment with depth in Subunit IIB and Unit III (Fig. 5). Nevertheless, even at 286 mbsf in almost pure chalk, the interstitial water is still depleted in ^{87}Sr compared with the marine composition of the carbonates.

In systems of slowly accumulating sediments, Ca is removed from the sediment and Mg is continuously added from seawater as an effect of diffusional exchange (e.g., Perry et al., 1976). For the same reason, H_2O uptake in hydrous minerals is not visible and the Cl content of the fluid does not change significantly. The low water/rock ratio estimated for the alteration of the tufts implies some chemical and mineralogical consequences for the evolution of the system. The pH value increases with depth (7.8 to 9.0), similar to those described in basalt dissolution experiment at 0°C are also observed (Crovisier, 1989). The alteration of about 20 wt% of the initial basaltic glass

should deliver 2000 to 4000 mmol of Ca to the interstitial fluid. Calcium is reprecipitated *in situ* in phillipsite, clinoptilolite, and calcite (Karpoff et al., this volume), but the average Ca content of the sediment is 7 wt% (on dry total), which implies a significant extraction of calcium if the initial glass concentration was 10–12 wt%. Part of this loss corresponds to Ca incorporated in fracture fillings, which are abundant between 50 and 150 mbsf and contain mainly a strange Ca-rich mineral named thaumasite (Karpoff et al., this volume). Thaumasite is also demonstrated to be the dominant sink for SO_4 on the basis of $\delta^{34}\text{S}$ of interstitial water (Alt and Burdett, this volume). Another consequence of the low water/rock ratio should be low Mg enrichment. Mg/Al molar ratios are between 0.9 and 1.1 in the 83–179 mbsf interval (pelagic clay excepted) compared with 0.94 to 1.9 in the volcaniclastic sediments of Sites 800 and 801.

CONCLUSIONS

Studies of the chemistry and Sr isotope composition of interstitial water at Sites 800, 801, and 802 have revealed patterns related to the alteration of volcanic matter under conditions in which diffusive exchange with seawater is low. At Sites 800 and 801 and in volcaniclastic turbidites at Site 802 (Unit V), diagenetic reactions are limited and no Cl increase is observed. At Site 802, the alteration of the Miocene tufts induces water uptake in secondary minerals and a subsequent Cl rise. The composition of the volcanic sediment is roughly similar at the three sites; however, Site 802 shows some distinctive characteristics: lower temperature, high cementation, probably high accumulation rates, and younger age (Miocene for Site 802 and middle to Late Cretaceous for the volcaniclastic turbidites at Sites 801, 801, and 802). Both high accumulation rates and cementation favor a “closed system” alteration of the tuff since the deposition of the sediment. In contrast, at Sites 800 and 801, prior to the development of chert sequences that sealed the system, no low-diffusion layer are present, and a low accumulation rate favored the high water/rock ratio alteration of the volcaniclastic sediment. This suggests that the volcaniclastic material at Sites 800 and 801 becomes almost “inert” compared with the Miocene tufts at Site 802.

The ages of the deposits are also an important factor in diffusion processes and it is possible that the gradients presently observed in the Miocene tuffs will be smoothed in 100 m.y., which is the age difference between the Miocene tuffs at Site 802 and the turbidites at Site 800.

ACKNOWLEDGMENTS

Support for research was provided by a grant from CNRS ASP "Soutien ODP-France." "Un grand merci" to Valerie Clark and Scott Chaffey in the chemistry lab of the *JOIDES Resolution*, Danielle Dautel, and Luc Marin for chemical help, Louis Derry for "frenghish" deciphering and various scientific discussions, and Peter Vrolijk, Andy Fisher, and an anonymous reviewer for constructive comments. This is CRPG contribution no. 887.

REFERENCES

- Alibert, C., Michard, A., and Albarède, F., 1983. The transition from alkali basalts to kimberlites: isotope and trace element evidence from melilitites. *Contrib. Mineral. Petrol.*, 82:176–186.
- Bird, P., 1984. Hydration-phase diagrams and friction of montmorillonite under laboratory and geologic conditions, with implications for shale compaction, slope stability, and strength of fault gouge. *Tectonophysics*, 107:235–260.
- Blanc, G., and ODP 135 Shipboard Scientific Party, 1991. Hydrogeochemistry of the Lau backarc basin and the Tonga forearc basin, ODP 135. *Terra Abstract*, 3:466.
- Burst, J. F., 1976. Argillaceous sediment dewatering. *Annu. Rev. Earth Planet. Sci.*, 4:293–318.
- Clauer, N., Hoffert, M., Grimaud, D., and Millot, G., 1975. Compositions isotopiques du Sr d'eaux interstitielles extraites de sédiments récents: un argument en faveur de l'homogénéisation isotopique des minéraux argileux. *Geochim. Cosmochim. Acta*, 39:1579–1582.
- Clauer, N., Hoffert, M., and Karpoff, A. M., 1975. The Rb-Sr isotope system as an index of origin and diagenetic evolution of southern Pacific red clays. *Geochim. Cosmochim. Acta*, 46:2659–2664.
- Collot, J.-Y., Greene, H. G., Stokking, L. B., et al., 1992. *Proc. ODP, Init. Repts.*, 134: College Station, TX (Ocean Drilling Program).
- Crovisier, J. L., 1989. Dissolution des verres basaltiques dans l'eau douce: essai de modélisation [Thèse de Doctorat]. Univ. Louis Pasteur, Strasbourg.
- Crovisier, J. L., Honnorez, J., and Eberhart, J. P., 1987. Dissolution of basaltic glass in seawater: mechanism and rate. *Geochim. Cosmochim. Acta*, 51:2977–2990.
- Dunoyer de Segonzac, G., 1970. The transformation of clay minerals during diagenesis and low-grade metamorphism: a review. *Sedimentology*, 15:281–346.
- Egeberg, P. K., Aagaard, P., and Craig Smalley, P., 1990a. Major element and oxygen isotope studies of interstitial waters: ODP Leg 113. In Barker, P. F., Kennett, J. P., et al., *Proc. ODP, Sci. Results*, 113: College Station, TX (Ocean Drilling Program), 135–146.
- Egeberg, P. K., and the Leg 126 Shipboard Scientific Party, 1990b. Unusual composition of pore water found in the Izu-Bonin fore-arc sedimentary basin. *Nature*, 344:215–218.
- Gieskes, J. M., 1976. Interstitial water studies, Leg 33. In Schlanger, S. O., Jackson, E. D., et al., *Init. Repts. DSDP*, 33: Washington (U.S. Govt. Printing Office), 563–570.
- Gieskes, J. M., and Johnson, J., 1981. Interstitial water studies, Leg 61. In Larson, R. L., and Schlanger, S. O., *Init. Repts. DSDP*, 61: Washington (U.S. Govt. Printing Office), 603–605.
- Gieskes, J. M., Vrolijk, P., and Blanc, G., 1990. Hydrogeochemistry of the Northern Barbados Accretionary Complex transect: Ocean Drilling Project Leg 110. *J. Geophys. Res.*, 95:8809–8818.
- Gislason, S. R., and Eugster, H. P., 1987. Meteoric water-basalt interaction I: a laboratory study. *Geochim. Cosmochim. Acta*, 51:2827–2840.
- Hanshaw, B. B., and Coplen, T. B., 1973. Ultrafiltration by a compacted clayey membrane. II: Sodium ion exclusion at various ionic strengths. *Geochim. Cosmochim. Acta*, 37:2311–2327.
- Hawkesworth, C. J., and Elderfield, H., 1978. The strontium isotopic composition of interstitial waters from Sites 245 and 336 of the Deep Sea Drilling Project. *Earth Planet. Sci. Lett.*, 40:423–432.
- Hoffert, M., Karpoff, A.-M., Clauer, N., Schaaf, A., Courtois, C., and Pautot, G., 1978. Néoforrations et altérations dans trois faciès volcanosédimentaires du Pacifique Sud. *Oceanol. Acta*, 1:187–202.
- Holland, H. D., 1978. *The Chemical Evolution of the Atmosphere and Oceans*: Princeton, NJ (Princeton Univ. Press).
- Kastner, M., and Gieskes, J. M., 1976. Interstitial water profiles and sites of diagenetic reactions, Leg 35, DSDP, Bellinghausen abyssal plain. *Earth Planet. Sci. Lett.*, 33:11–20.
- Koepnick, R. B., Burke, W. H., Denison, R. E., Hetherington, E. A., Nelson, H. F., Otto, J. B., and Waite, L. E., 1985. Construction of the seawater $^{87}\text{Sr}/^{86}\text{Sr}$ curve for the Cenozoic and Cretaceous: supporting data. *Chem. Geol. (Isot. Geosci. Sect.)*, 58:55–81.
- Koepnick, R. B., Denison, R. E., Burke, W. H., Hetherington, E. A., and Dahl, D. A., 1990. Construction of the Triassic and Jurassic portion of the Phanerozoic curve of seawater $^{87}\text{Sr}/^{86}\text{Sr}$. *Chem. Geol. (Isot. Geosci. Sect.)*, 80:327–349.
- Lancelot Y., Larson, R. L., et al., 1990. *Proc. ODP, Init. Repts.*, 129: College Station, TX (Ocean Drilling Program).
- Lawrence, J. R., and Gieskes, J. M., 1981. Constraints on water transport and alteration in the oceanic crust from the isotopic composition of pore water. *J. Geophys. Res.*, 86:7924–7934.
- Ludden, J. N., Gradstein, F. M., et al., *Proc. ODP, Init. Repts.*, 123: College Station, TX (Ocean Drilling Program).
- Manheim, F. T., and Sayles, F. L., 1974. Composition of interstitial waters of sediments, based on deep-sea drill cores. In Goldberg, E. D. (Ed.), *The Sea* (Vol. 5): New York (Wiley), 527–568.
- McDuff, E., 1981. Major cation gradients in DSDP interstitial water: the role of diffusive exchange between seawater and upper oceanic crust. *Geochim. Cosmochim. Acta*, 34:105–120.
- McDuff, E., and Gieskes, J. M., 1976. Calcium and magnesium profiles in DSDP interstitial waters: diffusion or reaction? *Earth Planet. Sci. Lett.*, 33:1–10.
- Mottl, M. J., and Gieskes, J. M., 1990. Chemistry of water sampled from Oceanic Basement Borehole, 1979–1988. *J. Geophys. Res.*, 95:9327–9342.
- Muelenbach, K., 1980. The alteration and aging of the basaltic layer of the sea floor: oxygen isotope evidence from DSDP/IPOD Legs 51, 52, and 53. In Donnelly, T., Francheteau, J., Bryan, W., Robinson, W., Flower, M., Salisbury, M., et al., *Init. Repts. DSDP*, 51, 52, 53: Washington (U.S. Govt. Printing Office), 1159–1167.
- , 1986. Alteration of the oceanic crust and the ^{18}O history of seawater. In Valley, J. W., Taylor, H. P., and O'Neil, J. R., *Stable Isotope in High Temperature Geological Processes*. Mineral. Soc. Am., Rev. in Mineral. Ser., 16:425–444.
- Newman, A.C.D., 1987. The interaction of water with clay mineral surfaces. In Newman, A.C.D. (Ed.), *Chemistry of Clays and Clay Mineral* (Vol. 5): London (Longman Scientific and Technical), 237–274.
- Odum, H. T., 1951. Notes on the strontium content of seawater, celestite, radiolaria, and strontianite snail shells. *Science*, 114:211.
- Parson, L., Hawkins, J., Allan, J., et al., 1992. *Proc. ODP, Init. Repts.*, 135: College Station, TX (Ocean Drilling Program).
- Perry, E. A., Gieskes, J. M., and Lawrence, J. R., 1976. Mg, Ca and $\text{O}^{18}/\text{O}^{16}$ exchange in the sediment-pore water system, Hole 149, DSDP. *Geochim. Cosmochim. Acta*, 40:413–423.
- Sayles, F. L., and Manheim, F. T., 1975. Interstitial solutions and diagenesis in deeply buried marine sediments: results from the Deep Sea Drilling Project. *Geochim. Cosmochim. Acta*, 39:103–127.
- Smith, W.H.F., Staudigel, H., Watts, A. B., and Pringle, M. S., 1989. The Magellan Seamounts: Early Cretaceous record of the South Pacific isotopic and thermal anomaly. *J. Geophys. Res.*, 94:10501–10523.
- Tribble, J. S., 1990. Clay diagenesis in the Barbados Accretionary Complex: potential impact on hydrology and subduction dynamics. In Moore, J. C., Masche, A., et al., *Proc. ODP, Sci. Results*, 110: College Station, TX (Ocean Drilling Program), 97–110.
- Vrolijk, P., Fisher, A., and Gieskes, J., 1991. Geochemical and geothermal evidence for fluid migration in the Barbados accretionary prism (ODP Leg 110). *Geophys. Res. Lett.*, 18:947–950.

Date of initial receipt: 3 June 1991

Date of acceptance: 6 January 1992

Ms 129B-124

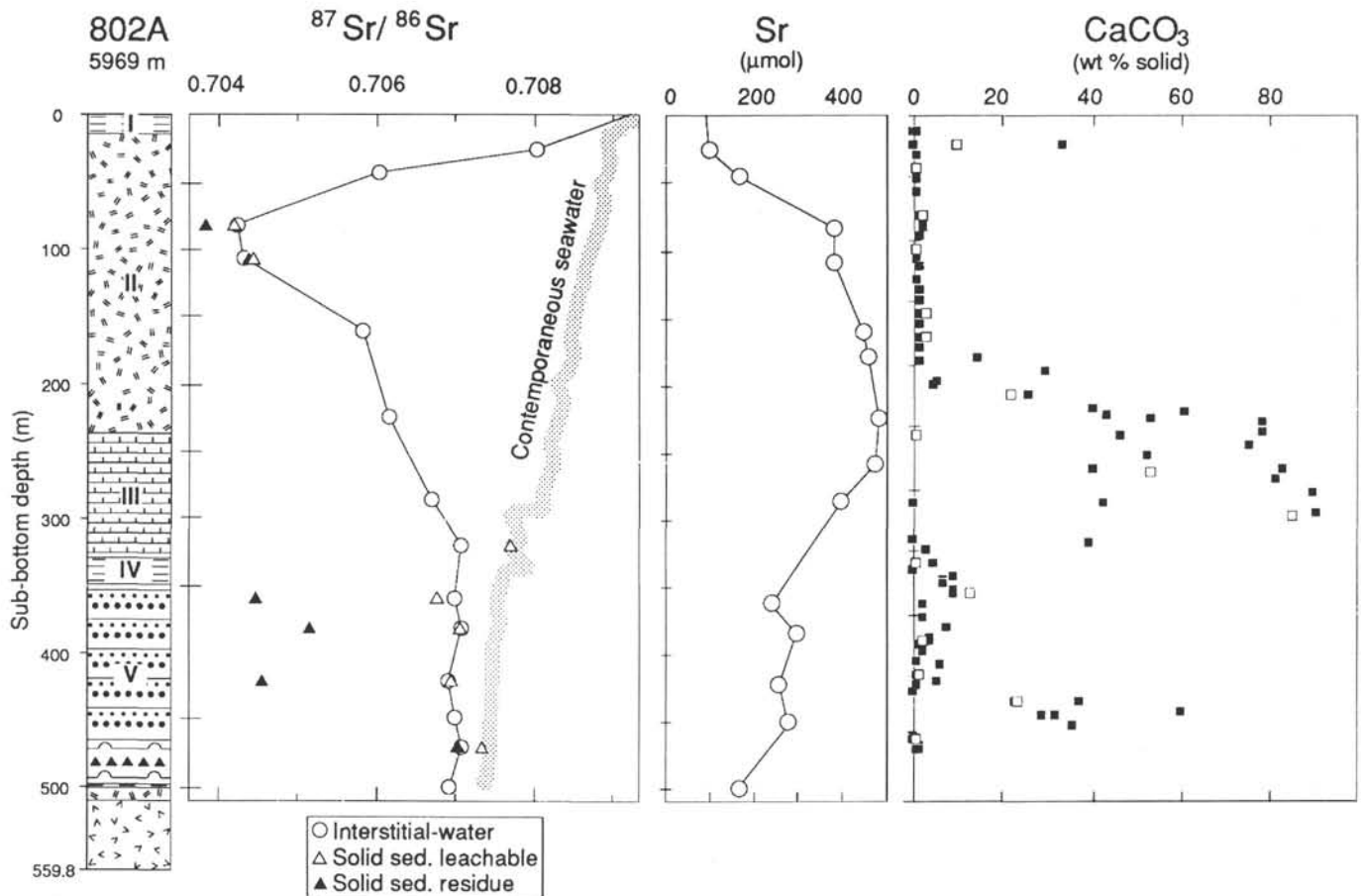


Figure 5. Site 802 distribution with depth of $^{87}\text{Sr}/^{86}\text{Sr}$ in pore fluids and in solid sediments, Sr in pore fluids, and CaCO_3 in solid sediment. Data are from Tables 1, 4, and 5 and Lancelot, Larson, et al. (1990). The contemporaneous seawater curve for Sr isotope ratio is drawn after Koepnick et al. (1985). Lithologic legend in Figure 4. Open symbols on the CaCO_3 plot are for the solid residue of interstitial water samples.

Table 2. Lithologic description and X-ray determination of major minerals of interstitial water sample sediment.

Core, section, interval (cm)	Depth ^a (mbsf)	Rock type	Quartz	Phillipsite	Clinoptilolite	Analcime	Calcite	Smectite	Volcanic minerals	Others
129-800A-										
4R-2, 25-30	22	Pelagic brown clay	x	xx	x	—	—	xx	o	Illite x
26R-2, 140-148	232	Volcaniclastic turbidite	xx	—	xx	—	x	xx	o	
27R-1, 140-150	239	Volcaniclastic turbidite	x	—	xxx	—	o	o	—	Celadonite xx
33R-6, 60-70	296	Volcaniclastic claystone	—	xx	—	—	xx	xxx	o	
37R-2, 0-10	327	Volcaniclastic claystone	—	—	—	—	—	xxxxx	—	
41R-2, 0-10	364	Volcaniclastic sandstone	—	—	—	—	—	o	xxxxx	—
49R-2, 140-150	434	Volcaniclastic siltstone	—	—	—	—	—	xxxxx	o	
54R-2, 0-12	473	Clayey radiolarite	xxxxx	—	—	—	—	xx	—	Hematite o
129-801A-										
3R-2, 145-150	15	Pelagic brown clay	x	x	—	—	—	xxx	—	Illite o
5R-3, 145-150	36	Pelagic brown clay	—	—	—	No data	—	—	—	
19R-1, 65-73	167	Siliceous silty claystone	o	—	x	—	o	x	—	Opal-CT xxxx
129-801B-										
5R-2, 0-10	225	Volcaniclastic silty claystone	o	—	xx	—	o	xxx	x	
8R-3, 115-125	257	Volcaniclastic silty claystone	xx	—	o	—	x	xxx	o	Celadonite o
33R-1, 143-150	436	Metalliferous red clay	xxxx	—	—	—	—	xx	—	Hematite x
35R-2, 0-10	446	Metalliferous red clay	xxx	—	—	—	—	xxx	—	Hematite x
129-802A-										
4R-1, 140-150	26	Brown volcanic ash-tuff	—	xx	o	—	x	xx	o	
6R-2, 0-10	44	Black volcanic ash-tuff	—	x	—	xxx	—	xxx	xx	Chabazite o
10R-2, 140-150	83	Black volcanic ash-tuff	—	—	—	No data	—	—	—	
13R-1, 53-58	109	Pelagic brown clay	—	o	xx	—	—	xxx	—	
19R-2, 107-117	162	Volcanic ash-tuff	—	xxx	—	x	—	xxx	xx	
21R-1, 103-110	179	Claystone	—	xxxx	—	o	—	xxx	xx	
26R-1, 0-10	225	Calcareous claystone	—	xx	—	—	xxx	x	xx	
29R-3, 29-34	258	Pelagic brown clay	o	o	xxx	—	x	xx	xx	
32R-2, 140-150	286	Nannofossil chalk	x	—	x	—	xxx	x	—	Opal-CT xx
36R-1, 80-88	322	Nannofossil chalk	—	—	o	—	xxxxx	—	—	Opal-CT x
40R-2, 140-150	361	Volcaniclastic turbidite	x	—	o	—	—	x	xxx	
43R-1, 140-150	384	Volcaniclastic turbidite	—	—	x	—	xx	xxx	xx	
47R-2, 140-150	422	Volcaniclastic siltstone	—	—	—	—	o	xxx	x	Celadonite x
50R-2, 140-150	450	Volcaniclastic silty claystone	—	—	xx	—	x	xxx	x	Celadonite o
53R-1, 120-130	471	Calcareous volcaniclastic claystone	xx	—	x	—	xx	x	o	
56R-2, 140-150	500	Volcaniclastic turbidite	—	—	—	—	o	xx	—	Sanidine xxx

Note: Qualitative estimates of the abundance based on peak height: xxxxx >90%, x = 5%, o = detected, — = not detected.

^aDepth rounded to the nearest meter.

Table 3. Major element composition of solid sediment (squeeze cake) in interstitial water samples.

Core, section, interval (cm)	Depth ^a (mbsf)	SiO ₂ (wt%)	Al ₂ O ₃ (wt%)	Fe ₂ O ₃ ¹ (wt%)	MnO (wt%)	MgO (wt%)	CaO (wt%)	Na ₂ O (wt%)	K ₂ O (wt%)	TiO ₂ (wt%)	P ₂ O ₅ (wt%)	Loss on ignition	Total (wt%)
129-800A-													
4R-2, 25-30	22	49.10	14.78	6.41	2.29	3.11	4.45	1.92	3.94	0.59	2.41	11.14	100.14
26R-2, 140-148	232	64.72	6.35	6.07	0.08	3.17	4.67	1.82	2.49	1.12	0.20	9.07	99.76
27R-1, 140-150	239	53.50	9.58	10.03	0.15	6.20	6.58	2.29	0.88	1.79	0.27	8.11	99.38
33R-6, 60-70	296	45.57	10.63	12.23	0.15	8.21	5.01	1.50	4.83	1.51	0.39	10.39	100.42
37R-2, 0-10	327	46.56	9.26	10.61	0.17	14.66	1.61	2.52	2.18	1.52	0.27	10.13	99.49
41R-2, 0-10	364	53.96	9.13	9.23	0.11	11.36	2.09	1.87	1.58	1.43	0.24	8.63	99.63
49R-2, 140-150	434	43.04	8.78	13.01	0.11	12.11	5.83	1.86	0.94	1.47	0.24	12.33	99.72
54R-2, 0-12	473	81.18	5.09	3.92	0.40	1.45	0.56	0.77	1.41	0.32	0.20	5.01	100.31
129-801A-													
3R-2, 145-150	15	49.56	16.82	7.34	2.15	3.27	1.85	2.09	4.15	0.61	1.04	11.43	100.31
5R-3, 145-150	36	54.46	15.13	6.04	0.96	2.97	1.75	2.09	4.27	0.55	0.98	10.51	99.71
19R-1, 65-73	167	63.62	6.76	6.40	0.08	3.67	4.76	1.97	2.16	1.36	0.26	9.24	100.28
129-801B-													
5R-2, 0-10	225	48.22	9.03	9.78	0.14	8.16	5.20	1.81	4.83	2.09	0.38	10.12	99.76
8R-3, 115-125	257	56.34	8.21	9.42	0.17	6.20	3.37	2.02	2.66	1.70	0.28	9.07	99.44
33R-1, 143-150	436	73.10	7.28	7.19	0.02	1.67	0.28	0.93	2.29	0.51	0.15	6.15	99.57
35R-2, 0-10	446	65.00	8.41	11.21	0.08	2.04	0.48	1.02	2.72	0.60	0.27	7.74	99.57
129-802A-													
4R-1, 140-150	26	40.23	9.80	10.35	0.07	8.76	7.76	3.29	2.00	2.75	0.35	14.31	99.67
6R-2, 0-10	44	43.65	10.50	11.98	0.15	10.73	3.20	4.91	0.86	2.77	0.36	9.33	98.44
10R-2, 140-150	83	41.92	11.03	12.55	0.17	8.36	5.41	4.70	0.29	3.08	0.41	11.57	99.49
13R-1, 53-58	109	48.87	11.50	7.69	1.58	3.02	4.19	2.88	1.58	0.65	0.75	16.87	99.58
19R-2, 107-117	162	43.67	10.16	11.58	0.17	9.73	7.13	3.72	1.04	2.47	0.32	9.74	99.73
21R-1, 103-110	179	43.32	10.71	11.13	0.15	8.38	6.44	3.97	1.51	2.62	0.36	10.28	98.87
26R-1, 0-10	225	37.59	9.89	8.60	0.20	4.47	14.98	2.61	1.72	1.53	0.27	17.70	99.56
29R-3, 29-34	258	52.71	10.96	8.33	2.02	2.88	3.55	2.70	1.63	0.51	0.83	13.63	99.75
32R-2, 140-150	286	27.75	3.41	1.62	0.45	0.86	33.42	0.72	0.41	0.16	0.56	29.91	99.27
36R-1, 80-88	322	6.61	1.31	0.58	0.14	0.44	49.04	0.08	0.03	0.08	0.40	40.18	98.89
40R-2, 140-150	361	49.53	11.60	12.96	0.12	5.19	6.22	2.45	1.64	3.18	0.44	6.37	99.70
43R-1, 140-150	384	43.45	8.21	8.80	0.16	6.12	11.89	1.95	1.63	2.42	0.30	14.40	99.33
47R-2, 140-150	422	49.25	9.35	11.10	0.14	11.21	4.39	2.17	0.55	2.50	0.32	8.76	99.74
50R-2, 140-150	450	51.34	9.48	10.55	0.19	10.19	2.75		1.04	2.50	0.27	9.62	100.09
53R-1, 120-130	471	48.15	7.94	5.77	0.07	2.22	15.30	1.56	1.20	0.97	0.25	16.73	100.16
56R-2, 140-150	500	55.14	11.55	9.07	0.04	4.44	1.28	1.29	7.00	0.97	0.12	8.95	99.85

Note: Fe₂O₃¹ as total iron.^aDepth rounded to the nearest meter.

Table 4. Carbonate content and trace element composition of solid sediment in interstitial water samples.

Core, section, interval (cm)	CaCO ₃ ^a (wt%)	B	Ba	C	Cr	Cu	Ni	Rb	Sr	Tb	V	Y	Zn	Zr
129-800A-														
4R-2, 25-30	0.6	141	400	256	51	385	581	86	269	13	127	503	201	154
26R-2, 140-148	5.3	29	60	15	122	79	46	36	493	<5	101	10	50	78
27R-1, 140-150	2	31	81	37	482	113	184	18	362	<5	168	17	83	127
33R-6, 60-70	8.2	55	61	32	374	82	167	48	105	<5	165	22	74	117
37R-2, 0-10	0.7	50	21	32	586	97	276	46	107	<5	98	12	86	111
41R-2, 0-10	1.2	38	18	41	623	111	265	31	134	<5	169	12	77	106
49R-2, 140-150	0.2	30	<5	43	791	25	276	17	124	<5	268	15	70	100
54R-2, 0-12	0.2	39	745	11	22	70	39	44	69	<5	42	10	82	54
129-801A-														
3R-2, 145-150		147	392	209	63	285	481	121	168	15	119	243	173	151
5R-3, 145-150		152	310	101	53	261	261	101	169	6	100	154	153	130
19R-1, 65-73		29	211	10	188	67	49	32	310	<5	110	13	67	114
129-801B-														
5R-2, 0-10	4.3	39	50	26	465	88	167	67	189	6	174	17	75	173
8R-3, 115-125	4	41	112	37	233	54	124	39	199	<5	136	12	71	126
33R-1, 143-150		51	214	523	60	77	71	73	79	<5	89	6	75	93
35R-2, 0-10		75	178	627	50	83	101	85	84	<5	138	16	101	108
129-802A-														
4R-1, 140-150	10	51	84	64	597	110	66.4	29	97	<5	258	26	82	182
6R-2, 0-10	0.7	47	61	51	648	123	298	12	123	<5	281	27	98	183
10R-2, 140-150	1.8	26	54	66	550	134	252	7	308	<5	295	29	101	203
13R-1, 53-58	0.5	56	229	167	45	322	259	29	1484	5	67	122	137	124
19R-2, 107-117	3	22	114	48	694	103	328	14	127	<5	258	24	93	161
21R-1, 103-110	2.7	28	94	60	487	112	280	19	158	<5	216	23	93	169
26R-1, 0-10	21.8	41	261	58	260	69	156	27	414	<5	204	24	76	101
29R-3, 29-34	0.4	112	886	75	31	332	81	30	780	5	126	138	157	113
32R-2, 140-150	53.5	37	454	21	15	88	67	16	676	13	19	76	56	31
36R-1, 80-88	85.4	24	442	7	12	48	17	13	494	16	7	52	17	13
40R-2, 140-150	0.5	41	108	27	313	140	119	28	391	6	274	29	141	204
43R-1, 140-150	13	35	68	3	470	114	209	26	303	<5	231	19	85	162
47R-2, 140-150	2.2	25	47	33	526	134	223	9	236	<5	257	19	96	166
50R-2, 140-150	1.7	31	185	52	767	122	230	14	294	<5	285	15	85	184
53R-1, 120-130	23.2	41	118	28	110	53	96	24	346	5	91	23	79	109
56R-2, 140-150	0.6	47	<5	45	161	119	93	78	53	<5	237	4	70	47

Notes: All analyses are in parts per million (ppm) except for CaCO₃, which is in weight percentage (wt%).^aShipboard analyses (Lancelot, Larson, et al., 1990).**Table 5. ⁸⁷Sr/⁸⁶Sr in solid sediments for the leachable fraction (carbonates) and the silicate residue.**

Core, section, interval (cm)	Silicate residue		Leachate	
	⁸⁷ Sr/ ⁸⁶ Sr	Sr (ppm)	⁸⁷ Sr/ ⁸⁶ Sr	Sr (ppm)
129-802A-				
10R-2, 140-150	0.703832 ± 17	49	0.704219 ± 31	658
13R-1, 53-58	0.704380 ± 37	1093	0.704458 ± 29	2452
36R-2, 80-88			0.707668 ± 23	457
40R-2, 140-150	0.704487 ± 14	292	0.706747 ± 23	347
43R-1, 140-150	0.705158 ± 27	217	0.707050 ± 21	202
47R-2, 140-150	0.704541 ± 27	121	0.706931 ± 17	267
53R-1, 120-130	0.707043 ± 21	227	0.707336 ± 34	403

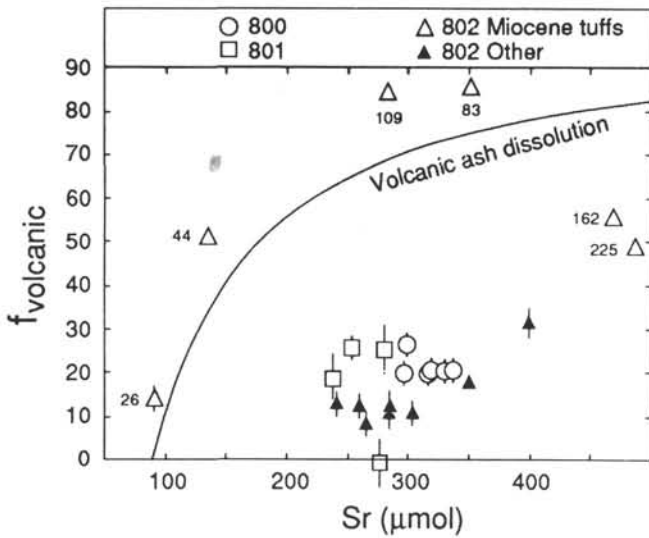


Figure 6. Sr content of interstitial water samples of the three sites vs. the fraction of volcanic Sr calculated from the Sr isotope ratio of pore water, contemporaneous seawater, and volcanic matter (see text). The vertical error bar corresponds to the uncertainty of the $^{87}\text{Sr}/^{86}\text{Sr}$ ratio of contemporaneous seawater. The curve corresponds to a dissolution of basalt in interstitial water. $^{87}\text{Sr}/^{86}\text{Sr}$ of volcanic matter has been taken at 0.7035, as it corresponds to average $^{87}\text{Sr}/^{86}\text{Sr}$ ratio of Cretaceous volcanism in the area (e.g., Smith et al., 1989; Castillo et al., this volume). Addition of biogenic Sr is necessary to explain the samples in which Sr is higher than expected for a given value of f_{volcanic} . The numbers with the Miocene tuff symbols (802) indicate the sub-bottom depth.

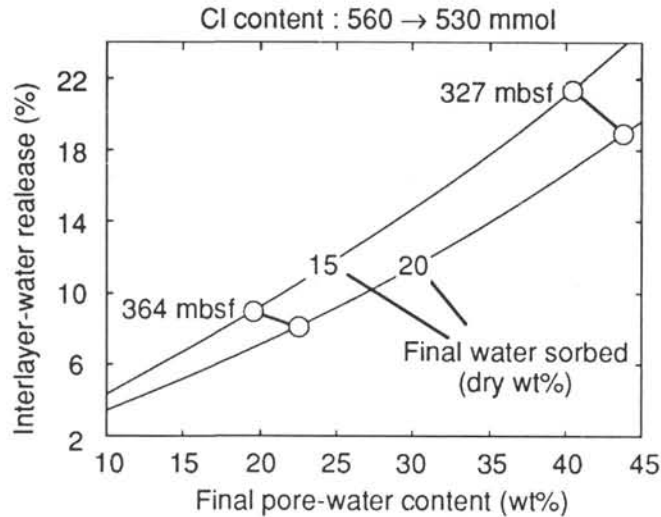


Figure 7. Estimate of interlayer-water dewatering for a 5.4% freshening of the pore water (560 → 530 mmol Cl) as a function of the final pore-water content of the sediment and the final interlayer water content of the smectite in a 90% smectite sediment. Interlayer-water dewatering corresponds to $(1 - I_{\text{final}}/I_{\text{initial}}) \cdot 100$. Points at 327 and 364 mbsf correspond to Samples 129-800A-37R-2, 0–10 cm, and 129-800A-41R-2, 0–10 cm, respectively, for which estimates of the pore-water content have been made from bulk water content measurements (France-Lanord and Sheppard, this volume).

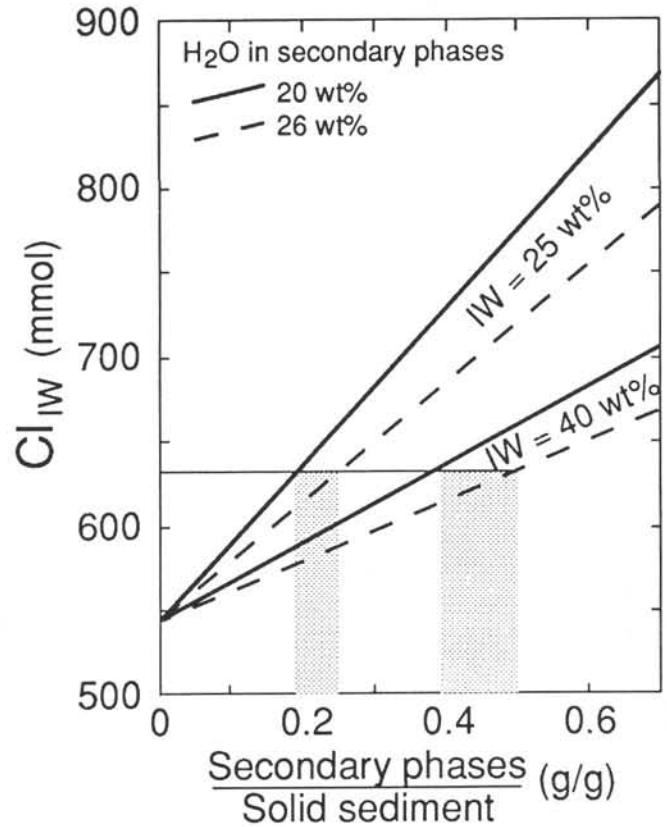


Figure 8. Chlorine increase by water uptake during alteration of a volcanoclastic sediment in a closed system. The initial fluid is seawater with 545 mmol Cl. The two line groups correspond to 25 and 40 wt% final water content in the sediment. Secondary phases contain 20 and 26 wt% of total water, which correspond to 0.25 and 0.35 g/g of water sorbed. The fraction of altered mineral is expressed as dry weight.